Validation of the AIRS Radiative Transfer Algorithm Using ECMWF Datafields

L. Larrabee Strow[a], Scott E. Hannon[a], S. De Souza-Machado[a], Howard Motteler[a]

[a]University of Maryland Baltimore County, Physics Department, Baltimore, Maryland 21228.

ABSTRACT

The Atmospheric Infrared Sounder (AIRS) was launched in early May 2002. This new high-spectral resolution sounder is the first of a new generation of temperature and humidity sounders for numerical weather prediction and climate change studies. In addition, AIRS should be able to detect several minor gases, including ozone, carbon monoxide, methane and carbon dioxide. This paper presents a preliminary comparison between observed AIRS spectra and spectra computed from the ECMWF (European Center for Medium Range Forecasting) model fields. A key component of this comparison is the selection of clear fields of view, which we limited to night views over ocean, allowing the use of the relatively well known sea surface emissivity.

1. INTRODUCTION

The Atmospheric Infra-Red Sounder (AIRS)[1] was launched into polar orbit on board NASA's AQUA platform on May 4, 2002. This high resolution instrument uses a complex physically-based algorithm for the retrieval of atmospheric profiles, and consequently is dependent on an accurate, and fast, radiative transfer algorithm for computing clear-air radiances. Assuming that the forward model accuracy approaches the noise level of the instrument, the high spectral resolution of AIRS coupled with its low noise should produce retrievals that are as good, or better, than the worldwide operational radiosonde network, especially for moisture.

An overview of the AIRS instrument is given in Aumann,[1] while details of the AIRS spectral calibration important for validating the AIRS radiative transfer algorithm (AIRS-RTA) are given in Strow.[2] AIRS covers the spectral range between 650 cm^{-1} (15 μm) to 2700 cm^{-1} (3.7 μm) using 2378 channels. The SRFs of these channels have full widths at half maximum of $\sim \nu/1200$, and noise levels on the order of 0.2K for a 250K scene temperature.

In this paper, we present an overview of observations of the atmospheric component of the AIRS radiances taken on June 14, 2002 and July 20, 2002, two days of data when the instrument and the AQUA platform were available for science observations. We concentrate on clear fields of view, which we limited to night views over ocean, allowing the use of the relatively well known sea surface emissivity. The observed spectra are compared to spectra computed from the ECMWF (European Center for Medium Range Forecasting) model fields.

A small bias between AIRS observations and computed radiances computed is generally only possible if (1) the AIRS radiances are radiometrically correct, (2) the AIRS spectral response functions (SRFs) used to simulate the AIRS radiances are accurate, (3) the ECMWF model fields are statistically accurate, and (4) the AIRS radiative transfer algorithm and underlying spectroscopy is correct. In this issue Aumann and Pagano[3] present a prelimary analysis of the AIRS sea surface radiances that suggests radiometric accuracy of at least 0.5K with the possiblity of accuracies approaching 0.2K. The results shown here support this conclusion. The narrow AIRS SRFs were well characterized during pre-launch calibration,[2] except for (1) the SRF center frequency which is easily determined empirically from the observed radiances, and (2) for small residual effects of fringing in the SRFs that is unimportant for most channels. In-flight calibration

Further author information: Send correspondence to LLS : E-mail: strow@umbc.edu

has recently successfully determined the fringing parameters, which will be included in the next AIRS-RTA, but are not included in the results presented in this paper. The ECMWF model fields are generally acknowledged to be the best global NWP fields. Although there has been much progress in atmospheric spectroscopy in recent years, uncertainties remain in characterizing the water vapor continuum, and the wings of the strong CO_2 bands, both of which are important for AIRS retrievals.

A key component of this work is the identification of clear fields of view over ocean at night. Our technique for detecting clear observations is only weakly dependent on the absolute accuracy of the AIRS radiometry, although it does require accurate relative (with wavenumber) radiometric calibration. Details on clear detection are discussed below. Our goal is to avoid significant clouds, and to minimize the effects of uncertain surface properties on our analysis of the atmospheric portion of the observed radiances.

2. RADIATIVE TRANSFER AND SPECTROSCOPY

The AIRS-RTA accuracy is determined by (1) the spectroscopy used to compute atmospheric transmittances, and (2) the quality of the fast model transmittance parameterization. A review of the basic form of the AIRS-RTA parameterization and it's accuracy is presented in.[4]

The monochromatic radiance leaving the top of a non-scattering, clear atmosphere is

$$\begin{aligned} R_\nu &= \epsilon_\nu B_\nu(T_s)\tau_\nu(p_s\rightarrow 0,\theta_{\rm sat}) \\ &+ \int_{p_s}^{0} B_\nu\left(T(p)\right)\frac{d\tau_\nu(p\rightarrow 0,\theta_{\rm sat})}{dp}dp \\ &+ F_d^\nu \rho_{\rm th}\tau_\nu(p_s\rightarrow 0,\theta_{\rm sat}) \\ &+ \frac{H^\nu(\theta_{\rm sun})}{\sec(\theta_{\rm sun})}\tau_\nu(0\rightarrow p_s,\theta_{\rm sun})\rho_{\rm solar}\tau_\nu(p_s\rightarrow 0,\theta_{\rm sat}). \end{aligned} \quad (1)$$

The first term is the surface blackbody emission where ϵ_ν is the surface emissivity and $B_\nu(T_s)$ is the Planck function. The second term is the atmospheric emission, followed by the downwelling atmospheric emission reflected by the surface. F_d^ν is the downwelling thermal flux and $\rho_{\rm th}$ the reflectance of this flux by the surface, which we assume to be Lambertian. Reflected solar radiation is represented by the last term in this equation, where $H^\nu(\theta_{\rm sun})$ is the solar irradiance incident at the top of the atmosphere and $\rho_{\rm solar}$ is the solar reflectance by the surface. $\tau_\nu(p\rightarrow 0,\theta_{\rm sat})$ is the atmospheric layer-to-space transmittance from some pressure p to space along the satellite zenith angle $\theta_{\rm sat}$.

The observed AIRS radiance for channel i is the convolution of the monochromatic radiance, R_ν, with the normalized instrument SRF for channel i,

$$robs_i = \int_{\Delta\nu_i} R_\nu\, SRF_i(\nu)\, d\nu. \quad (2)$$

The AIRS forward model uses a discretized version of Eq.1 for each spectral channel i, using 100 atmospheric layers l, which is sufficiently fine to keep discretization errors below the AIRS noise level. The transmissions for the AIRS channels are rapidly computed using a set of predictors, that were obtained by using 48 regression profiles. We refer the interested reader for details about the parameterization of the gas transmittances, via the predictors used for the fast model, to Strow.[4]

The monochromatic transmittances for each of the 48 regression profiles were calculated using the kCARTA[5,6] atmospheric radiative transfer code, and included all gases contained in the 2000 HITRAN database. kCARTA code includes CO_2 P/R-branch mixing at both 4.3 and 15 microns, and a newly derived H_2O continuum in the strong 6 micron water band. Elsewhere kCARTA uses the CDK2.4 continuum.

While kCARTA does have the capability of performing scattering computations, as well as simple non-LTE computations, the AIRS-RTA was designed for use only in clear sky cases. We have validated the radiative transfer in kCARTA with field data from various aircraft campaigns,[7] such as CAMEX1, WINTEX

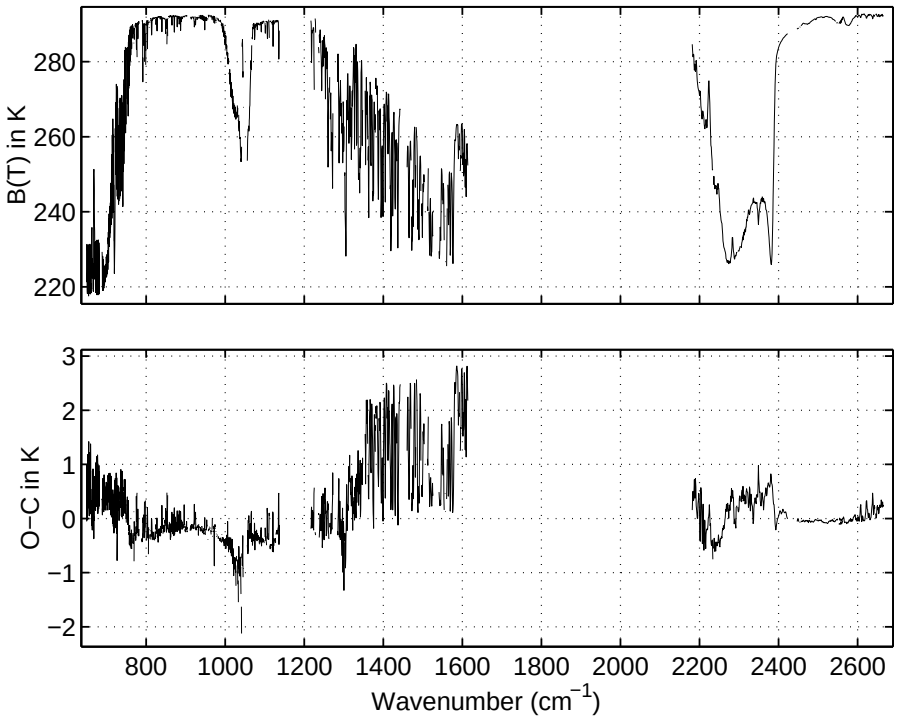

Figure 1. AIRS bias spectrum for clear FOVS in 3 granules on July 20, 2002. Computed spectrum uses kCARTA and ECMWF model fields.

and CLAMS. Using kCARTA as the "truth" for the development of the AIRS-RTA, typical regression profile errors are below the AIRS noise levels.[4]

kCARTA is unique in it's inclusion of P/R-branch line-mixing in CO_2, which redistributes the radiation of overlapping spectral lines away from what would be computed using non-interacting Lorentz lineshapes. Line-mixing reduces the effective far-wings of these interacting lines, while increasing the lineshape near the line centers. Duration-of-collision effects also considerably reduce the CO_2 line wing from Lorentz values, and is especially important in the head of the ν_3 band near 2400 cm^{-1} (4.3 μm) that contains excellent temperature sounding channels. kCARTA also includes Q-branch line-mixing for Q-branches. While some line-by-line algorithms contain Q-branch line-mixing, we are not aware of any other line-by-line algorithms that explicitely treat P/R-branch line-mixing.[7,8]

kCARTA uses the CKD2.4[9] continuum, except inside the strong 6.7 micron water band, where we have developed a different continuum based on recent laboratory results. This new continuum improves comparisons to observations made with aircraft-borne infrared interferometers such as the University of Wisconsin's SHIS and the NPOESS NAST instrument. Comparisons between the observed spectra from the CAMEX-1, WINTEX and CLAMS campaigns, against simulations using a water vapor continuum developed by Strow[4,10] show more consistent agreement in this spectral region (see below).

kCARTA actually computes monochromatic transmittances and/or radiances from compressed look-up tables of atmospheric transmittances, resulting in very fast computation times. kCARTA is extensively documented[6] and is available from the authors.

The kCARTA look-up table transmittances are computed with a custom line-by-line (LBL) algorithm developed by the authors, called UMBC-LBL. The only real requirement on the UMBC-LBL is to compute kCARTA's static look-up tables of compressed transmittances. These tables only change when improvements are made to the molecular line parameters or gas cross-sections, an infrequent occurance. Since speed is not an important issue for UMBC-LBL we can accurately model both Q-, and P/R-branch mixing

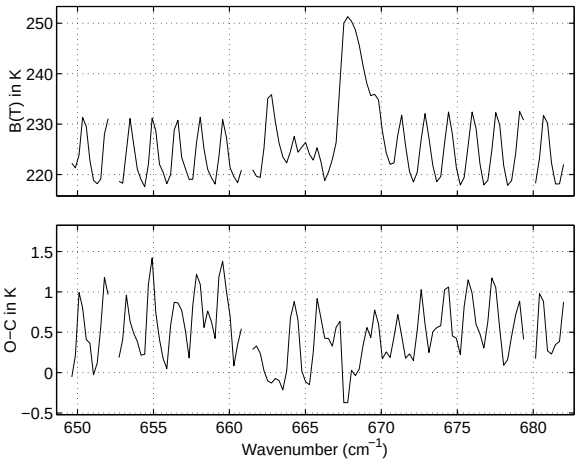

Figure 2. Zoom of Fig. 1 in the region dominated by high-altitude CO_2 emission.

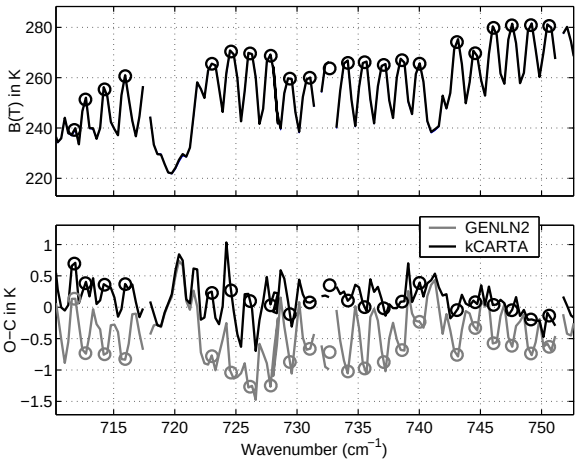

Figure 3. Zoom of Fig. 1 in the region dominated by mid-tropospheric CO_2 emission.

in UMBC-LBL, and not rely on perturbation solutions. At present UMBC-LBL includes CO_2 line-mixing for 12 Q-branch and 12 P/R-branch bands. The P/R-branch bands also include a duration-of-collision term discussed earlier. A detailed description of UMBC-LBL is available.[11]

In the following results it is important to differentiate between two different radiative transfer algorithms (RTAs) used here. Since kCARTA is a monochromatic RTA, we can easily compute AIRS radiances on any spectral grid. This is not the case for the AIRS fast radiative transfer model used for profile retrievals (the AIRS-RTA), which requires extensive (2-weeks) computation of parameters for any particular set of AIRS channel centroids. During the initial phases of AIRS operation the channel centers can shift, depending on the instrument temperature (the channel centers are very stable when the instrument is in operational mode). Fortunately, for the data presented here the AIRS operating channel centers were only displaced by ∼1-3% of the SRF width from the existing AIRS-RTA channel centers, which will produce computed brightness temperature errors on the order of ±0.6K in the 15 micron CO_2 band. However, we have also updated the kCARTA spectroscopy since the AIRS-RTA was last generated. Changes include an updated continuum in the 1250-1620 cm^{-1} region, producing brightness temperature differences of up to ∼3K, and changes to the CO_2 lineshape in the 2200 - 2400 cm^{-1} region on the order of 2K. Both of these changes to kCARTA are based on new laboratory results.

3. RESULTS

3.1. Detection of Clear Fields of View

The selection of clear observations is a two-step process. We first select fields of view (FOVs) for which the average brightness temperature of all adjacent FOVS are within 0.25K of the center FOV. This test is done for several window channels in both the 10 and 3.8 micron regions. This test discriminates against partly cloudy scenes or scenes with highly variable water vapor. In the second step, we require that the sea surface temperature derived from channels in the 10 and 3.8 micron window regions are identical within some threshold, generally about 0.4K. This lessens our dependence on absolute accuracy in the AIRS radiometric calibration, but does require that the relative AIRS radiometric calibration be accurate, which was demonstated during ground calibration. This technique also assumes that we have good knowledge of the sea surface emissivity, and most importantly, that the ECMWF water fields and the water vapor spectroscopy (continuum) are both accurate enough to remove the effects of atmospheric emission when deriving sea surface temperatures, especially in the 10 micron window. Finally we require the observed sea surface temperatures to agree with the ECMWF model temperatures to within 4K, a very loose requirement that discriminates against low uniform cloud decks.

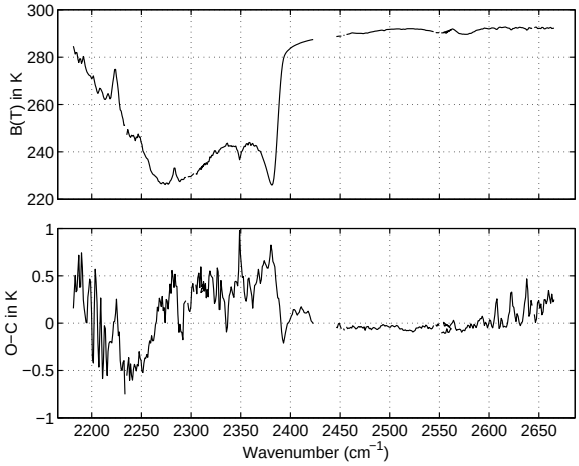

Figure 4. Zoom of Fig. 1 in the 4.3 micron region dominated by CO_2 emission.

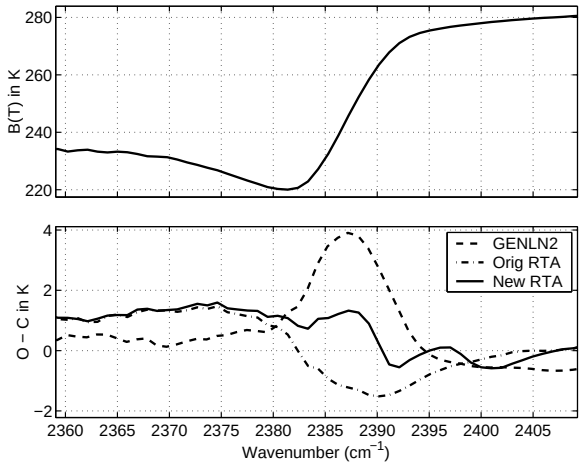

Figure 5. The bottom panel shows bias calculations for three different models of the CO_2 line wing. See the text for details.

We have not to date performed a rigorous error analysis of this procedure. We do find that only a very small percentage of ocean, night FOVs satisfy these requirements, but enough to obtain good statistics. A modified version of this test for daylight observations that does not use the 3.8 micron region of the spectrum shows very good visual correlation with apparently clear FOVs in the AIRS 3-color visible imagery (with approximate spatial resolution of 2 km).

These clear tests were applied to the global set of night, ocean AIRS radiances from July 20, 2002 between ±50 degrees latitude. The *median* observed - calculated bias at 2616 cm^{-1} (the best AIRS window channel) was -0.18 ± 0.2K, and at 900 cm^{-1} was -0.11 ± 0.5K. The quoted error bars are statistical errors only, and do not include possible errors in the ECMWF model sea-surface temperature, in the sea-surface emissivity, in the water vapor continuum, or in the ECMWF water fields. However, these are very reasonable results and, in any case, provide us with FOVs that do not exhibit significant cloud radiative effects, allowing us to concentrate on biases in the atmospheric emission. There is reason to expect small negative biases in these window regions because of (1) small amounts of un-detected cloud, and (2) the evaporative cooling of the emitting ocean skin layer at night.

Most of the results shown below do not use this global data set, but instead uses clear FOVs detected in three nightime granules (a granule is a 90 x 135 grid of AIRS FOVs) denoted by the AIRS Science Team as “focus granules” for July 20. The main reason to restrict most of our bias calculations to 3 graunles is because it reduces the amount of clear FOVs, allowing us to use the much slower kCARTA RTA which can perform radiance calculations at the correct channel center frequences. In addition, as mentioned above, kCARTA also contains more up-to-date spectroscopy. For these 3 granules the 2616 cm^{-1} bias is -0.16K and the 900 cm^{-1} bias is -0.04K. Since these granules average over a much smaller sampling of the ECMWF sea-surface fields, we expect higher errors in the window biases due to regional biases in the ECMWF sea-surface temperatures.

3.2. Bias Spectra Relative to ECMWF Model Fields

We now present a sample of comparisons between AIRS observations and kCARTA/AIRS-RTA simulations. The ECMWF profiles are on a 0.5 x 0.5 degree latitude/longitude grid. We have access to eight daily grids, some of which are analysis fields, while the others are 3 or 6 hour forecast fields. We chose the ECMWF grid point closest to the AIRS observations in space and time. Similar bias calculations were performed for a limited amount of AIRS observations using the NCEP fields. These results indicated that the NCEP and ECMWF temperature fields gave very similar biases, in the CO_2 emission regions, while the ECMWF water

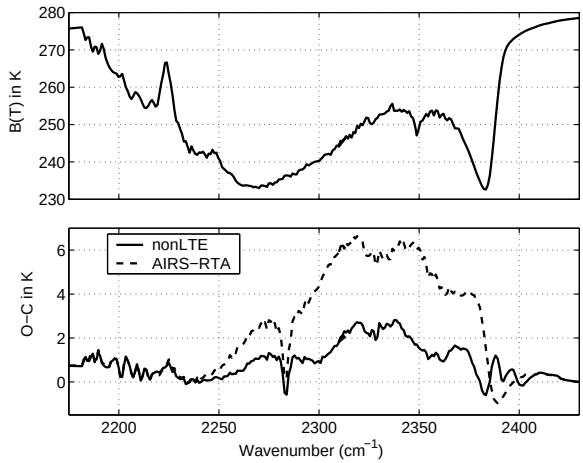

Figure 6. Non-local thermodynamic emission in the 4.3 micron region. The RTA used in the dashed curve in the bottom panel does not include non-LTE. The solid curve uses a simple model of non-LTE in kCARTA.

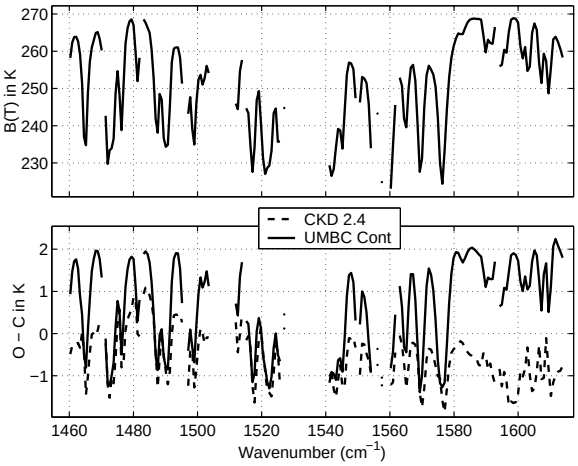

Figure 7. Bias in the region of strong H_2O emission using ECMWF water fields with the CDK2.4 continuum and a new continuum derived by the authors.

fields generally produced lower biases in the H_2O emission regions than the NCEP fields. Consequently, we have concentrated here on validation with the ECMWF fields. A more systematic study of the NCEP vs ECMWF water fields is certainly warranted.

The kCARTA results shown here are a snapshot of the spectroscopy in kCARTA during the summer of 2002. We are actively analyzing laboratory data of both CO_2 and H_2O to improve our lineshape and continuum models. For example, very early examination of AIRS biases versus ECMWF indicated errors in the difficult to model 2380-2400 cm^{-1} region of CO_2. Subsequent examination of the laboratory data we used to parameterize line-mixing and duration-of-collision effects in this spectral region (a two-parameter fit) showed that most of the AIRS biases in this region was caused by very small (0.04 in absolute transmittance) deviations between the laboratory data in this region and our lineshape model. During the initial analysis of the laboratory data, it was difficult to attribute these difference to either the theory or the data.

Figure 1 shows the AIRS brightness temperature mean bias spectrum (Obs - Calc) for the clear FOVs in three granules recorded on July 20, 2002. The agreement between computed and observed brightness temperatures is clearly excellent, especially in regions dominated by CO_2. The largest biases are in the H_2O region from 1300 to 1600 cm^{-1}. This is not unexpected given the difficulty in modeling water vapor in NWP models, and the high spatial and temporal variability in water. However, this water region bias appears persistant in data from other days, and may be indicative of a model bias. We generally have smaller biases in-between the water lines in this region in comparisons between radiosonde measurements and co-located observations with high-altitude aircraft radiance observations using NAST and SHIS. However, the line core biases are smaller for AIRS than NAST/SHIS, presumably because the radiosonde measurements are poor for higher altitude water, while the ECMWF model fields are more based on satellite measurements.

The second largest biases are near the coldest regions of ozone emission, suggesting that some combination of either the ECMWF ozone amounts or temperature near the top of the ozone layer are in error. Figure 2 is a zoom of Fig. 1 in the region dominated by high-altitude CO_2 emission at 15 microns. In-between the lines we see that the biases are in the range of 0 to 0.25K, with higher biases of about 1K at the line centers. The line centers are emitting in the stratosphere, where the ECMWF model fields are known have a cold bias on the order of ~0.5-1K.[12] These results indicate that the AIRS radiometric and spectral calibration, and the RTA spectroscopy are accurate to at least 0.5K.

Figure 3 is another zoom of Fig 1, where we have also added the bias using the line-by-line code GENLN2.[13] kCARTA was initially based on GENLN2, and the differences between the kCARTA and GENLN2 biases are due to the inclusion of P/R-branch line-mixing in kCARTA. This is especially apparent in-between the spectral lines, marked by circles in this figure. Again, the biases are between 0 to 0.5K in this region as well.

The CO_2 emission in the shortwave region (4 microns) has traditionally been difficult to model because of the rather extreme effects of line-mixing and duration-of-collision effects on the R-branch bandhead near 2400 cm^{-1}. Overall we see bias errors of ±0.5K, but with some systematic deviations with wavenumber. The +0.5K bias around the center of the band at 2350 cm^{-1} is possibly due to the cold bias of the ECMWF fields in the stratosphere. At lower wavenumbers the bias becomes negative, which could be due to a number of factors, including an inaccurate CO_2 line-wing, inaccurate N_2O amounts in the RTA, and possibly the ECMWF fields. The 15 micron CO_2 region does not have any negative biases, so there is an incompatibility between these two spectral regions that cannot be only due to inaccuracies in the ECMWF temperature fields. The structure in the bias between 2175 and 2225 cm^{-1} is likely due to two factors. First, this region is sensitive to carbon monoxide, which is known to vary significantly in space and time. Second, the AIRS SRFs in this spectral region is quite sensitive to the residual fringing, which is not included in this calculation. We have recently shown the inclusion of fringing effects (which required in-orbit testing to parameterize) reduces the variability in the bias in this spectral region.

The original AIRS-RTA (fast model) was based on a parameterization of line-mixing and duration-of-collision effect using laboratory spectra. As discussed earlier our initial parameterization produced observed minus computed transmittance errors of up to 0.04, which is quite small compared to the overall magnitude of these effects. The bottom panel of Fig. 5 shows the bias for the original RTA (max error of ~ -1.5K), the bias for GENLN2 (max error of ~ 4K), and the bias for our modified lineshape model (max error of about 1K). This modified lineshape model is a re-fit of the laboratory data to our model, where we allow the two parameters controlling line-mixing and duration-of-collision to vary slowly with wavelength. This result shows the power of AIRS observations coupled with the ECMWF model to uncover spectroscopic uncertainties. The spectral region centered around 2380 cm^{-1} may also have some small biases due to uncertainties in about 5 AIRS SRFs, since the SRF line-wing must be determined very accurately due to the sharp rise in radiances in the wing.

Figure 6 shows the *daytime* biases for clear FOVS in a single granule. The bottom panel shows that there are large differences in the 2250 - 2380 cm^{-1} region, using the current AIRS-RTA model, which assumes all molecules are in local thermodynamic equilibrium (LTE) at all levels in the atmosphere. The same panel shows that a simple modification to the spectroscopic and radiative transfer model, using a non-LTE model for atmospheric layers above 60 km for the main CO_2 00011 band,[14] reduces the errors from 7 K down to about 2 K. The vast majority of channels in this spectral region are not needed for temperature sounding, so this effect does not need to be modeled correctly for the standard AIRS products.

The determination of the source of biases in regions dominated by water vapor will be challenging, since water vapor is highly variable both spatially and temporally, and is difficult to account for accurately in NWP models. In addition, water vapor spectroscopy is also difficult, especially determination of the water vapor continuum (a parameterization of the water vapor line wings). Moreover, radiosondes are historically quite inaccurate above 300 mbar, so NWP models often depend more on satellite data in this region than on radiosonde data.

Figure 7 is a zoom of Fig. 1 in the strong part of the H_2O band. The solid line in the bottom panel is the bias using a new continuum developed at UMBC from new laboratory data of water vapor. We have shown that this new continuum improves the biases between high-altitude aircraft observations of high-resolution radiances and radiances computed from both radiosonde measurements and ECMWF model fields (unpublished work). The dashed line in this plot is the bias using the CKD2.4 continuum.[9] Clearly the CKD continuum gives lower biases. However, a close examination of these biases indicates that the CDK2.4 bias spectrum is inconsistent. Figure 8 is a scatterplot of the biases in Fig. 7 where the

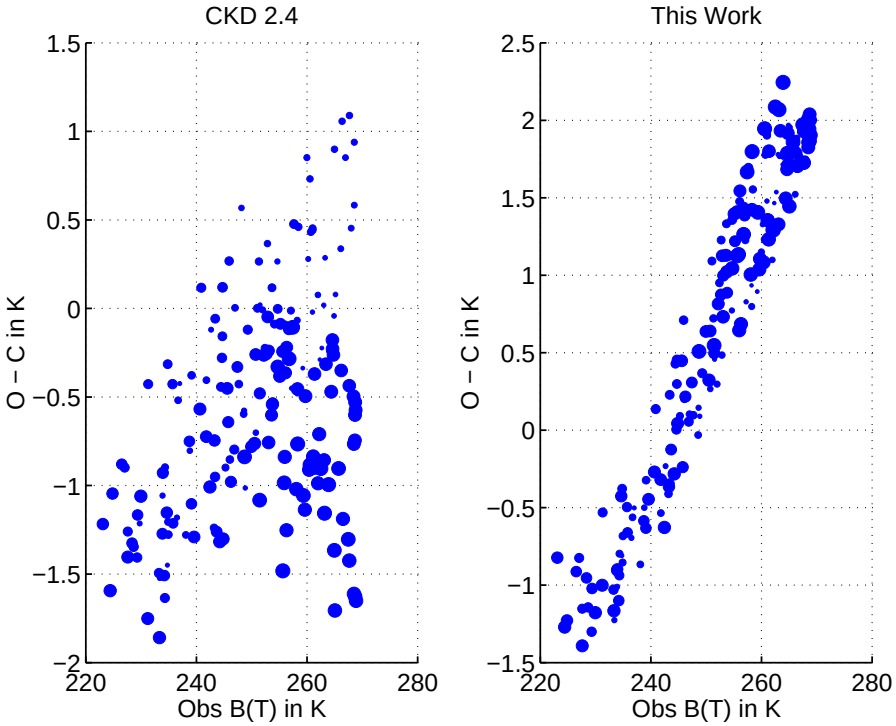

Figure 8. Scatterplot of the data shown in Fig. 7. The observed brightness temperature is a proxy for the weighting function of the emission. The large scatter for the CKD data indicates that CDK2.4 is inconsistent as a function of wavenumber. The size of the circles reflects the wavenumber, which varies from 1450 to 1620 cm^{-1}.

biases are plotted versus the observed brightness temperatures, which is a rough proxy for the peak of the weighting function for each channel. In this region, channels with the same brightness temperature should have similar biases, *if* the error source is the ECMWF water fields. The left panel in Fig. 8 shows that the CKD2.4 bias varies considerably for the same observed brightness temperature, while the same scatterplot for our new continuum contains significantly less scatter for a given observed brightness temperature. This indicates that our new continuum is much more consistent than CDK2.4, and that at least some of the observed bias errors are probably due to the ECMWF water fields.

A complete analysis of the AIRS water biases is far beyond the scope of this paper, and may ultimately only be understood with data from the AIRS validation effort[15] that will include a number of co-located radiosonde launches and water vapor lidar measurements.

4. CONCLUSIONS

This paper provides a first look comparison between observed AIRS radiances and radiances simulated using ECMWF data fields. The overall agreement between the AIRS observed radiance and radiances computed using ECMWF fields is remarkable, especially for observations made so early in the AQUA-AIRS mission. Observed biases in the colder CO_2 regions of ~0.5K or lower suggests that the AIRS radiometric calibration is quite accurate. Moreover this work also shows that both the AIRS forward model and the ECMWF fields are reasonably accurate. Much work remains to validate the AIRS foward model for water vapor, both in the strong H_2O band and in the window regions where the water vapor continuum must be well characterized in order to derive sea surface temperatures.

Future work will also include analysis of the global variability of minor gases that can be detected with AIRS radiances, including CO_2, CH_4, and CO. AIRS may also provide new information on non-LTE emission in the upper atmosphere, something that has never been measured globally by a nadir viewing

instrument. Work has just begun on studying the effects of clouds on spectral radiances. For example, AIRS should excel at detecting thin cirrus clouds because of the almost continuous wavelength coverage in the 10-12 micron atmospheric window.

Finally, these results suggest that the AIRS instrument, and the AIRS-RTA, are ready for use by the NWP community to help improve medium range forecasts and will become a very useful tool for climate studies.

Acknowledgments

The authors thank the European Center for Medium Range Forecasting (ECMWF) for use of forecast and analysis model fields. This work was supported by NASA Contract NAS5-31378. The authors also acknowledge significant contributions by Dave Tobin (University of Wisconsin/SSEC) to the CO_2 and H_2O lineshape models used in this paper,

REFERENCES

1. H. Aumann, M. Chahine, C. Gautier, M. Goldberg, E. Kalnay, L. McMillin, H. Revercomb, P. Rosenkranz, W. Smith, D. Staelin, L. Strow, and J. Susskind, "AIRS/AMSU/HSB on the Aqua mission: Design, science objectives, data products and processing systems," *IEEE Transactions on Geosciences* , 2002. accepted for publication in the IEEE Transactions on Geoscience and Remote Sensing.
2. L. Strow, S. Hannon, M. Weiler, K. Overoye, S. Gaiser, and H. Aumann, "Pre-launch spectral calibration of the atmospheric infrared sounder (AIRS)," *IEEE Transactions on Geosciences* , 2002. accepted for publication in the IEEE Transactions on Geoscience and Remote Sensing.
3. "First results from airs on the eos," in *Proceedings of the SPIE EUROPTO Remote Sensing Crete, September 2002, Crete, Greece*, 2002.
4. L. Strow, S. Hannon, S. D. Machado, and H. Motteler, "An overview of the AIRS radiative transfer model," *IEEE Transactions on Geosciences* , 2002. accepted for publication in the IEEE Transactions on Geoscience and Remote Sensing.
5. L. Strow, H. Motteler, R. Benson, S. Hannon, and S. De Souza-Machado, "Fast computation of monochromatic infrared atmospheric transmittances using compressed look-up tables," *jqsrt* **59**(3-5), pp. 481–493, 1998.
6. S. De Souza-Machado, L. L. Strow, H. Motteler, and S. Hannon, "kCARTA: An atmospheric radiative transfer algorithm using compressed lookup tables," tech. rep., University of Maryland Baltimore County, Department of Physics, http://asl.umbc.edu/rta/lbl.html, 2002.
7. S. DeSouza-Machado, L. Strow, D. Tobin, H. Motteler, and S. Hannon, "Improved atmospheric radiance calculations using CO_2 P/R-branch line mixing," in *Proceedings of the European Symposium on Aerospace Remote Sensing Europto Series*, September 1999.
8. D. C. Tobin, *Infrared Spectral Lineshapes of Water Vapor and Carbon Dioxide*. PhD thesis, University of Maryland Baltimore County, 1996.
9. S. A. Clough, M. J. Iancono, and J. L. Moncet, "Line-by-line calculations of atmospheric fluxes and cooling rates: application to water vapor," *J.Geophys.Res.* **97**, pp. 15,761–15,785, 1992.
10. L. Strow, D. Tobin, W. McMillan, S. Hannon, W. Smith, H. Revercomb, and R. Knuteson, "Impact of a new water vapor continuum and line shape model on observed high resolution infrared radiances," *J. Quant. Spectrosc. Rad. Trans.* **59**(3-5), pp. 303–317, 1997.
11. S. De Souza-Machado, L. L. Strow, D. Tobin, H. Motteler, and S. Hannon, "UMBC-LBL: An algorithm to compute line-by-line spectra," tech. rep., University of Maryland Baltimore County, Department of Physics, http://asl.umbc.edu/rta/kcarta.html, 2002.
12. A. McNally, 2002. private communication.
13. D. Edwards, "Genln2: A general line–by–line atmospheric transmittance and radiance model," *NCAR Technical Note 367+STR*, National Center for Atmospheric Research, Boulder, Colo., 1992.
14. D. P. Edwards and M. Lopez-Puertas, "Non lte studies of 15 um bands of co2 for atmospheric remote sensing," *J.Geophys.Res.* **98**, pp. 14955–14977, 1993.

15. E. Fetzer, L. McMillin, M. Goldberg, S. Zhou, H. Ding, D. Tobin, D. Whiteman, J. Barnes, J. Yoe, M. Newchurch, D. Hagan, M. Hofstadter, P. Minnett, R. Bennartz, W. McMillan, R. Atlas, F. Schmidlin, H. Vomel, V. Walden, and H. Revercomb, "AIRS/AMSU/HSB validation," *IEEE Transactions on Geosciences* , 2002.